Probing Electronic States of Ne_2^+ and Ar_2^+ by Measuring Kinetic-Energy-Release Distributions

J. Fedor,* R. Parajuli,† S. Matt-Leubner, O. Echt,‡ F. Hagelberg,§ K. Głuch,‖ A. Stamatovic,¶ M. Probst, P. Scheier, and T. D. Märk**

Institut für Ionenphysik, Leopold Franzens Universität, Technikerstrasse 25, A-6020 Innsbruck, Austria

(Received 14 February 2003; published 26 September 2003)

Dissociative decay of metastable, electronically excited neon and argon dimer ions produces fragment ions with strikingly dissimilar kinetic-energy-release distributions. The distributions have been modeled based on *ab initio* calculations of potential energy curves. The unusual bimodal distribution observed for dissociation of Ne_2^+ arises from competition between radiative and nonradiative decay of the long-lived $II(1/2)_u$ state. For Ar_2^+, however, electronic predissociation is insignificant.

DOI: 10.1103/PhysRevLett.91.133401 PACS numbers: 36.40.–c, 31.50.Df, 33.70.Ca, 34.50.Gb

Homonuclear rare gas dimer ions continue to attract wide interest. They occur in high-pressure plasmas; their presence may constitute a major loss factor in rare gas excimer lasers [1]. They affect the optical properties and fragmentation dynamics of rare gas cluster ions [2,3], and they serve as model systems for investigations of fundamental phenomena such as tunneling through light-induced molecular potentials [4]. The potential curves for the six lowest lying electronic states have been computed by a variety of *ab initio* approaches (see, e.g., Refs. [5–7] for Ar_2^+ and [8,9] for Ne_2^+). Various spectroscopic methods, most notably photoelectron-photoion coincidence techniques, have produced a plethora of data that pertain to the ground and excited electronic states [10–13]), but many details are still unknown. Most experiments sample only certain regions of the potential curves, for example, those that are accessible by vertical transitions from the neutral or charged dimer near their equilibrium separations.

So far, the only observations of metastable decay reactions $R_2^+ \rightarrow R^+ + R$ (R = rare gas atom) pertain to argon. The metastability of Ar_2^+ on the time scale of $\approx 10\ \mu$s had originally sparked a controversial discussion [14,15]. The mechanism prevalent for metastability in atomic clusters, namely, vibrational predissociation, cannot be operative in two-atomic systems. Three other mechanisms, radiative decay, tunneling through a barrier, or electronic predissociation (radial coupling), had been proposed to account for the metastable dissociation of Ar_2^+ [14]. Whitaker *et al.* [6] suggested that it arises from the radiative decay of Ar_2^+ $II(1/2)_u$ into $I(1/2)_g$ (see Fig. 1 for the qualitatively similar potential energy curves of Ne_2^+). Electronic predissociation has been inferred from optical emission spectra of $HeNe^+$ [16].

In this contribution we show that high-resolution kinetic energy distributions of monomeric fragment ions that are formed in the decay of long-lived excited electronic states of isolated Ar_2^+ and Ne_2^+ are sensitive probes for potential curves and the rates of transitions between the corresponding electronic states. Combined with an *ab initio* study, the experimental data reveal that the $II(1/2)_u$ state in Ne_2^+ decays not only via the radiative channel suggested for Ar_2^+ and the heavier rare gas dimer ions [6,12], but also by electronic predissociation into $I(3/2)_u$. This is the first time that electronic predissociation has been established for a low-lying electronic state of a homonuclear rare gas dimer ion. As for $HeNe^+$ [16], the transition is unusual because there is no curve crossing between the initial and the final state.

The apparatus consists of a high-resolution double focusing three-sector field mass spectrometer of BEE geometry (magnetic analyzer followed by two electrostatic analyzers) [17]. Rare gas dimers are produced by expanding either neon or argon through a nozzle into vacuum. Expansion conditions for neon were nozzle diameter 10 μm, stagnation pressure 5 bars, and stagnation temperature $-170\,^\circ$C. The corresponding values for argon were 20 μm, 1 bar, and $-150\,^\circ$C, respectively. The

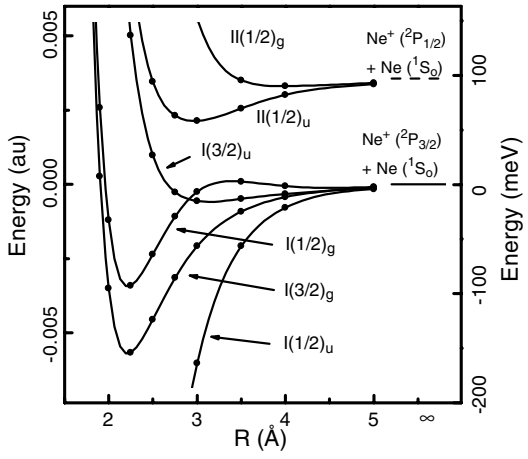

FIG. 1. Presently calculated potential curves for Ne_2^+, based on *ab initio* calculations [9] with spin-orbit interaction added. Curves are labeled by the projection of the total electronic angular momentum on the molecular axis Ω and parity [Hund's case (c)]. The potential curves for Ar_2^+ are qualitatively similar.

ensuing neutral dimers are ionized by electron impact. Although supersonic expansion of rare gases may lead to formation of larger clusters which, upon ionization, could decay into the dimer ion [3,18], the expansion conditions given above are such that the dimer ion signal is not contaminated by fragments from larger clusters [10,19]. The ions are extracted by an electric field and accelerated by 3 kV into the spectrometer. They are momentum analyzed by a magnetic sector field, energy analyzed by a 90° electric sector field, enter a field-free region (length 92 cm), pass through another 90° electric sector field, and are detected by a channeltron. The pressure in the field-free region, where decay reactions are analyzed, is kept well below 10^{-7} mbar under typical experimental conditions, ensuring that collision-induced dissociation is negligible [6].

MIKE (Mass-Analyzed Ion Kinetic Energy) spectra are measured to investigate decay reactions of mass-selected ions [17,20]: The magnet and first electric sector are tuned to pass the parent ion m_p, while the second electric sector field voltage U is scanned. Stable singly charged dimer ions will have a kinetic energy of 3 keV and pass at the nominal voltage of $U_p = 510$ V. Monomer ions (mass $\frac{1}{2}m_p$), formed between the two electric sectors in a spontaneous decay reaction of a dimer ion, will then pass at a voltage $U_f = \frac{1}{2}U_p$.

In Fig. 2 (open circles) we show the MIKE peak of metastable Ar_2^+ decaying into $Ar^+ + Ar$. The shape and width reflect the kinetic energy release (KER) of the reaction. Basically, the KER scales as the square of the width of the MIKE peak. The distribution of the total kinetic energy released in the center-of-mass system, KERD, is obtained by taking the derivative of the MIKE peak (properly deconvoluted with the shape of the Ar_2^+ parent peak) and transforming the sector field voltage to kinetic energies in the center of mass [17,21]. As shown in Fig. 3 (dashed curve), the KERD rises sharply from 0, reaches a maximum at about 1 meV, and then decreases slowly. The average KER of this distribution amounts to 19 meV. For comparison, Whitaker *et al.* estimated an average of 55 meV [6], but their procedure did not involve a complete analysis of the KERD.

The starting point for our computational work is the neutral Ar_2 dimer. We use the semiempirical potential of Barker *et al.* [22] to compute the rovibrational energy levels; their population is assumed to be thermal. We further assume that rotational and vibrational temperatures T are identical [23]. For each rovibrational level, we compute the Franck-Condon factor for vertical transition (caused in the experiment by electron impact) into rovibronic states of Ar_2^+, assuming $\Delta J = 0$, i.e., no change in the angular momentum of the nuclear system. The potential curves $V(r)$ for the excited states of Ar_2^+ are taken from *ab initio* calculations by Whitaker *et al.* [6] and Gadea and Paidarova [7]. Cubic splines are used to derive analytical expressions from the discrete sets of data.

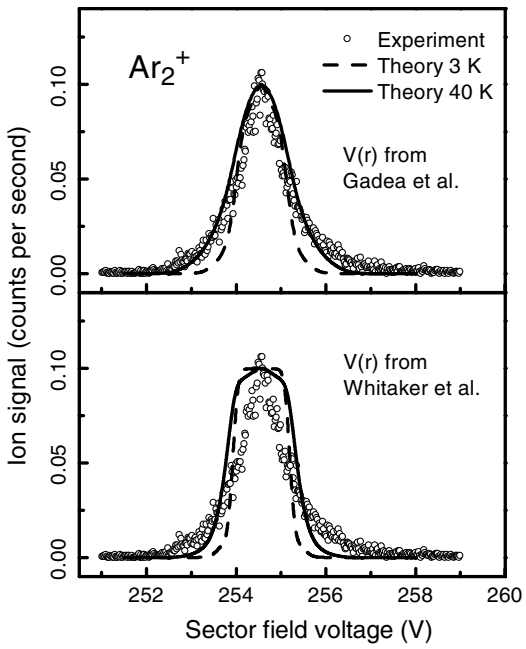

FIG. 2. Open circles: scan of electric sector field voltage revealing the formation of Ar^+ from metastable decay of Ar_2^+ (MIKE scan). Both panels display the same experimental data. The lines are derived from computed kinetic-energy-release distributions (KERD) based on *ab initio* potential curves reported by Gadea and Paidarova [7] (top panel) and Whitaker *et al.* [6] (bottom panel). The rovibrational temperature T of the neutral precursor, Ar_2, serves as the only adjustable parameter.

We thus arrive at a population of the rovibronic Ar_2^+ states . In agreement with results by Whitaker *et al.* [6], the $II(1/2)_u$ state is found to be one of the most strongly populated electronic states. For each of its (v, J) levels we compute the matrix element for radiative transitions into lower lying electronic states subject to the selection rule $\Delta J = 0, \pm 1$. Transitions into the $I(1/2)_g$ continuum have

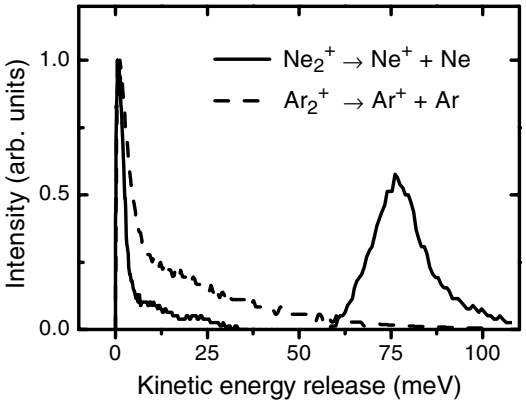

FIG. 3. Kinetic-energy-release distributions for the metastable dissociation of Ar_2^+ (dashed curve) and Ne_2^+ (solid curve), derived from the experimental MIKE peaks shown in Figs. 2 and 4, respectively.

rates of order 10^0 to 10^4 s^{-1}, with a rather large dependence on (ν, J). Transitions into the $I(3/2)_g$ state proceed with much smaller rates, in agreement with the $\Delta\Omega = 0$ propensity rule, and transitions into states of *ungerade* parity are dipole forbidden.

For each radiative transition from $II(1/2)_u(\nu, J)$ into the $I(1/2)_g$ continuum we evaluate the KER as the energy difference between the continuum level and the asymptotic energy of $I(1/2)_g$. This KER is weighted with the probability that the $II(1/2)_u(\nu, J)$ state is initially populated, times the probability that the transition will occur in the experimental time window. Summing over all transitions we arrive at a theoretical kinetic-energy-release distribution (KERD). Comparison with experiment can now be based on the KERD (Fig. 3) that was obtained by deconvoluting and differentiating the experimental MIKE peak. Alternatively, we can apply the reverse procedure to the theoretical KERD and compare the result with the experimental raw data shown in Fig. 2. We choose the latter method because convoluting is a more robust procedure than deconvoluting somewhat noisy experimental data.

In Fig. 2 we compare the experimental MIKE peak with theoretical MIKE peaks (lines) based on *ab initio* potential curves reported by Gadea and Paidarova [7](top panel) and Whitaker *et al.* [6](bottom panel). The rovibrational temperature T of the neutral precursor, Ar_2, serves as the only adjustable parameter. Good agreement between experiment and theory is obtained for the potential curves reported by Gadea, for $T = 40$ K. This T value is close to values that have been measured for Ar_2 by Raman scattering [23], and estimated for larger clusters based on the concept of evaporative cooling [24].

On the other hand, the agreement between experiment and theory is poor when calculations are based on the potential curves reported by Whitaker *et al.* [6]. This suggests that these curves are less accurate than those reported by Gadea and Paidarova [7], in agreement with results of a recent comparison of calculated and experimental values for equilibrium separations and well depths for excited states in Ar_2^+ [13]. We have systematically modified the potential curves in order to analyze how they affect the theoretical MIKE peaks [25]. It appears that an overestimation of the local maximum in the $I(1/2)_g$ state in Whitaker's work [6] causes the discrepancy with our experimental data. Decay into the repulsive part of that local maximum implies elevated KER values and a depletion of very small KER values, thus leading to the nearly flattopped theoretical MIKE peak shown in Fig. 2, bottom panel.

The MIKE peak of metastable decay of Ne_2^+ into $Ne^+ + Ne$ is shown in Fig. 4. The spectrum differs strikingly from that of argon; it appears to have two components. The KER distribution derived from the MIKE peak (Fig. 3, solid line) is bimodal. The low-energy part is qualitatively similar to the KERD measured for Ar_2^+, but its average value is only 6 meV. The other, broad and flattopped component in the MIKE spectrum corresponds to a KERD that is relatively narrow and peaks around 80 meV; see Fig. 3.

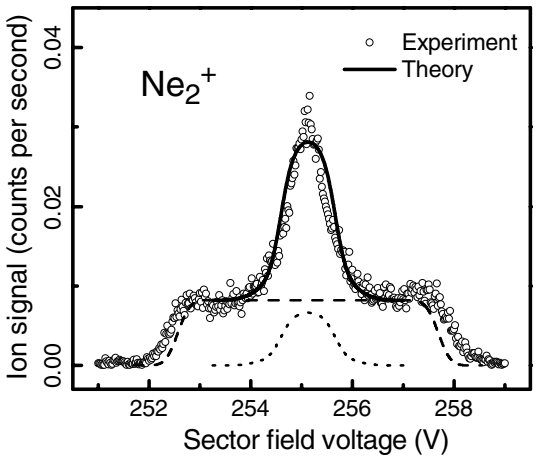

FIG. 4. MIKE scan of $Ne_2^+ \rightarrow Ne^+ + Ne$. The outer wings in the experimental spectrum indicate an additional, high-energy component in the KERD; see Fig. 3. The broken lines are derived from ab-initio potential curves (see Fig. 1) The narrow and broad components arise from radiative and non-radiative decay of $II(1/2)_u$, respectively. The solid line is obtained with the strengths of the two components being fitted separately.

To obtain theoretical MIKE spectra, we used high-level *ab initio* calculations for Ne_2^+ [9]. To these potential curves we have added the effect of spin-orbit coupling following the procedure described by Cohen and Schneider [26]. The results are shown in Fig. 1. Again, radiative bound-free transitions $I(1/2)_g \leftarrow II(1/2)_u$ feature lifetimes that roughly match the experimental time window ($10.7 \leq t \leq 13.4$ μs). We assumed a value of 10 K for the rovibrational temperature of the precursor, Ne_2, guided by the observation that the temperature of evaporating clusters scales as their binding energy [24]. The computed MIKE peak (dotted line in Fig. 4) accounts for the central part of the experimental MIKE peak reasonably well. The calculation was repeated with temperatures of 5 and 20 K (not shown), but the change in the shape of the computed MIKE spectrum is rather small.

However, the radiative $I(1/2)_g \leftarrow II(1/2)_u$ transition cannot account for the high-energy component in the KER distribution. The only process originating from the $II(1/2)_u$ state that could give rise to such a large kinetic energy release is a radiationless transition into an electronic state that converges to the $Ne(^1S_0) + Ne^+(^2P_{3/2})$ dissociation limit. The KER for this reaction would be restricted to $E_{so} - D_0 \leq \mathrm{KER} \leq E_{so}$ where $E_{so} = 96.8$ meV is the spin-orbit splitting in Ne^+, and D_0 is the dissociation energy of the local minimum in the $II(1/2)_u$ state.

For a more quantitative comparison, we have computed the matrix elements for radiationless transitions from

Ne_2^+ $II(1/2)_u$ into electronic states that converge to $Ne(^1S_0) + Ne^+(^2P_{3/2})$ along the lines of the predissociation theory presented by Carrington and Softley [16]. The strongest radiationless transition is into the continuum of $I(3/2)_u$. It proceeds chiefly by rotational coupling between the electronic and the nuclear degrees of freedom. A careful averaging over a range of rovibrational levels of the $II(1/2)_u$ state is essential. The KERD and the corresponding MIKE peak that arise from these transitions are computed as described above, starting from a thermal distribution of rovibrational states of Ne_2. The result is shown in Fig. 4 as a dashed curve. It matches the broad component quite well, although it is slightly narrower. This deviation points to an overestimation of the contribution from low-lying vibrational levels in the $II(1/2)_u$ state, or an overestimation of its well depth.

The solid line in Fig. 4 represents the sum of the two computed MIKE peaks that arise from radiative and nonradiative transitions, respectively. For this fit, the weight of the narrow component was increased from a computed value of 15% (used to plot the dotted line in Fig. 4) to 35%. However, the experimental data shown in Fig. 4 were recorded (in order to optimize the resolution) under conditions that discriminate against energetic fragment ions. A spectrum recorded in the second field-free region of the spectrometer features lower discrimination, but also lower resolution; it shows a weight of 22% for the narrow component, close to the computed 15%. Moreover, the computed values are quite sensitive to the assumed rotational temperature of the neutral neon dimer.

A similar calculation for Ar_2^+ $II(1/2)_u$ shows that its lifetime with respect to electronic predissociation is 2 orders of magnitude longer than that of Ne_2^+, explaining the absence of a high-energy component in the MIKE peak (Fig. 2), or the KER distribution (Fig. 3).

In conclusion, we have shown that the kinetic energy released in the metastable dissociation of Ar_2^+ and Ne_2^+ is sensitive to details of the potential curves that are involved in the electronic transitions. The experimental distributions are a sensitive probe of the details of the calculated potential curves, and they reveal the nature of the transition, i.e., radiative decay versus electronic predissociation.

The authors thank I. Paidarova for providing potential curves of Ar_2^+ and J. Harvey and J. Urban for fruitful discussions. This work was partly supported by the FWF, ÖAW, and ÖNB, Wien, Austria, the European Commission, Brussels, and NSF through the CREST program under HRD-9805465 and NSF-0132618.

*Permanent address: Department of Plasma Physics, Comenius University, SK-84215 Bratislava, Slovak Republic.
†Present address: Department of Physics, Amrit Campus, Tribhuvan University, Kathmandu, Nepal.
‡Permanent address: Department of Physics, University of New Hampshire, Durham, NH 03824, USA.
§Permanent address: Department of Physics, Atmospheric Sciences, and General Science, Jackson State University, Jackson, MS 39217, USA.
‖Permanent address: Institute of Mathematics, Physics and Informatics, Maria Curie-Sklodowska University, Lublin 20-031, Poland.
¶Permanent address: Faculty of Physics, P.O. Box 638, Yu-11001 Beograd, Yugoslavia.
**Corresponding author.
Also at Department of Plasma Physics, Comenius University, SK-84248 Bratislava, Slovak Republic.
Email address: tilmann.maerk@uibk.ac.at

[1] J. G. Eden, IEEE J. Sel. Top. Quantum Electron. **6**, 1051 (2000); H. Ninomiya and K. Nakamura, Opt. Commun. **134**, 521 (1997); G. N. Gerasimov *et al.*, Sov. Phys. Usp. **35**, 400 (1992).
[2] B. Von Issendorff *et al.*, J. Chem. Phys. **111**, 2513 (1999); R. B. Jones *et al.*, J. Chem. Phys. **102**, 4329 (1995); Z. Y. Chen *et al.*, J. Chem. Phys. **93**, 3215 (1990); M. J. Deluca and M. A. Johnson, Chem. Phys. Lett. **162**, 445 (1989).
[3] T. D. Märk and O. Echt, in *Clusters of Atoms and Molecules II*, edited by H. Haberland (Springer-Verlag, Berlin, 1994), Vol. 56, p. 154.
[4] C. Wunderlich *et al.*, Phys. Rev. A **62**, 023401 (2000).
[5] Y. Mizukami and H. Nakatsuju, J. Chem. Phys. **92**, 6084 (1990); W. R. Wadt, J. Chem. Phys. **68**, 402 (1978).
[6] B. J. Whitaker *et al.*, J. Chem. Phys. **93**, 376 (1990).
[7] F. X. Gadea and I. Paidarova, Chem. Phys. **209**, 281 (1996).
[8] N. Moiseyev *et al.*, J. Chem. Phys. **114**, 7351 (2001); J. Masik *et al.*, Int. J. Quantum Chem. **63**, 333 (1997).
[9] F. Y. Naumkin and D. J. Wales, Mol. Phys. **93**, 633 (1998).
[10] K. Norwood *et al.*, J. Chem. Phys. **90**, 2995 (1989).
[11] A. Carrington *et al.*, J. Chem. Phys. **116**, 3662 (2002); Y. C. Chiu *et al.*, J. Chem. Phys. **112**, 10 880 (2000); G. Ramos *et al.*, Phys. Rev. A **56**, 1913 (1997); T. Pradeep *et al.*, J. Chem. Phys. **98**, 5269 (1993).
[12] H. Yoshii *et al.*, J. Chem. Phys. **117**, 1517 (2002).
[13] P. Rupper and F. Merkt, J. Chem. Phys. **117**, 4264 (2002).
[14] K. Stephan and T. D. Märk, Phys. Rev. A **32**, 1447 (1985).
[15] A. J. Illies and M. T. Bowers, Org. Mass Spectrom. **18**, 553 (1983).
[16] A. Carrington and T. P. Softley, Chem. Phys. **92**, 199 (1985).
[17] S. Matt-Leubner, Int. J. Mass Spectrom. **222**, 213 (2003).
[18] T. D. Märk, Int. J. Mass Spectrom. **79**, 1 (1987); U. Buck and H. Meyer, J. Chem. Phys. **84**, 4854 (1986).
[19] A. J. Stace *et al.*, Chem. Phys. Lett. **184**, 113 (1991).
[20] R. G. Cooks *et al.*, *Metastable Ions* (Elsevier, Amsterdam, 1973).
[21] M. F. Jarrold *et al.*, J. Phys. Chem. **87**, 2213 (1983).
[22] J. A. Barker *et al.*, Mol. Phys. **21**, 657 (1971).
[23] H. P. Godfried and I. F. Silvera, Phys. Rev. A **27**, 3008 (1982).
[24] C. E. Klots, Nature (London) **327**, 222 (1987).
[25] J. Fedor, Physics Diploma thesis, Comenius University, Bratislava, 2003.
[26] J. S. Cohen and B. I. Schneider, J. Chem. Phys. **61**, 3230 (1974).